Sabkha dolomite as an archive for the magnesium isotope composition of seawater

Author(s):
Shalev, Netta; Bontognali, Tomaso R.R.; Vance, Derek

Publication date:
2021

Permanent link:
https://doi.org/10.3929/ethz-b-000463495

Originally published in:
Geology 49(3), https://doi.org/10.1130/g47973.1

Funding acknowledgement:
185988 - Using oceanic Mg and Sr stable isotope records to understand the past Earth (SNF)
184873 - Using trace metal isotopes to understand ocean biogeochemistry: ancient and modern (SNF)

Sabkha Dolomite as an Archive for the Magnesium Isotope Composition of Seawater

Netta Shalev[1], Tomaso R.R. Bontognali[123], and Derek Vance[1]

[1]*Institute of Geochemistry and Petrology, Dep. of Earth Sciences, ETH Zürich, Clausiusstr. 25, 8092 Zürich, Switzerland; netta.shalev@erdw.ethz.ch*

[2] *Space Exploration Institute, Fbg de l'Hopital 68, 2002 Neuchâtel, Switzerland*

[3]*Dep. of Environmental Sciences, Univ. of Basel, Klingelbergstr. 27, Basel, Switzerland*

ABSTRACT

Recent studies have uncovered the potential of Mg isotopes ($\delta^{26}Mg$) for studying past ocean chemistry, but records of such data are still scarce. Dolomite has been suggested as a promising archive for $\delta^{26}Mg$ of seawater. However, its enigmatic formation mechanism, and the difficulty in precipitating dolomite in the laboratory at surface temperatures, decreases confidence in the interpretation of $\delta^{26}Mg$ from the rock record. To evaluate factors determining the $\delta^{26}Mg$ of dolomite, we studied pore-water and sediment from Dohat Faishakh Sabkha, Qatar: one of the rare environments where dolomite is currently forming. The $\delta^{26}Mg$ values of the dolomite (-2.56‰ to -1.46‰) are lower than seawater (-0.83‰), whereas $\delta^{26}Mg$ values of pore-water (-0.71‰ to -0.14‰) are higher. The isotope fractionation accompanying dolomite formation is generally in accordance with an empirical fractionation from the literature, extrapolated to the Sabkha's temperature (-1.84‰ to -1.51‰). The results suggest that evaporated seawater is the sole source of Mg and isotopically light dolomite is the major sink, so that the $\delta^{26}Mg$ of the dolomite-forming pore-water is equal to or greater than that of seawater. Thus, provided that the lowest $\delta^{26}Mg$ value among several dolomite samples is used and the formation temperature is known, similar sabkha-type dolomites can be utilized as an archive for $\delta^{26}Mg$ values of ancient seawater.

INTRODUCTION

Reconstructions of the oceanic Mg budget are important to our understanding of the past Earth because important surface processes, such as weathering, mid-ocean ridge volcanism, and carbonate precipitation, control oceanic Mg inputs and outputs (e.g., Elderfield, 2010). Recent studies have shown the potential of Mg isotopes to enhance our understanding of the Mg budget of the past oceans (e.g., Tipper et al., 2006; Shalev et al., 2019). A few pioneer studies have produced Cenozoic seawater $\delta^{26}Mg$ records from Ca-

carbonate archives (Pogge Von Strandmann et al., 2014; Higgins and Schrag, 2015; Gothmann et al., 2017). However, the scarcity of such record data, and differences between existing datasets, currently limit this approach.

Dolomite, a common sedimentary rock constituted by the homonymous mineral $CaMg(CO_3)_2$, has been suggested as a promising archive for seawater $\delta^{26}Mg$, because Mg is a major element in dolomite and, therefore, it is less sensitive to post-depositional alteration than other substrates (e.g., Geske et al., 2012; Hu et al., 2017). However, the use of dolomite is more complicated than Ca-carbonate archives. For example, the $\delta^{26}Mg$ of marine-derived dolomite-forming solutions may be altered by contributions of Mg from sources other than seawater (e.g., Azmy et al., 2013), or by a Rayleigh distillation effect due to dolomite or Mg-evaporite precipitation (e.g., Li et al., 2011; Blattler et al., 2015; Shalev et al., in rev.). Furthermore, the mechanism of isotope fractionation between dolomite and its parent solution is not fully understood (e.g., Li et al., 2015). Many factors have been suggested to affect the isotope difference between dolomite and solution, $\Delta^{26}Mg_{dol\text{-}aq}$, including: temperature, aqueous speciation, precursor mineral formation, precipitation rate, and others (e.g., Geske et al., 2015a,b; Schott et al., 2016). In particular, because microbes and their extracellular polymeric substances (EPS) are considered to be an important catalyst for dolomite formation (Petrash et al., 2018), it is possible that the $\Delta^{26}Mg_{dol\text{-}aq}$ may also be influenced by biological factors.

Previous studies, aiming at quantifying $\Delta^{26}Mg_{dol\text{-}aq}$ values, have yielded a wide and often inconsistent range of results (e.g., Li et al., 2015). Higgins and Schrag (2010) suggested that $\Delta^{26}Mg_{dol\text{-}aq}$ is between -2.7 and -2.0‰ for deep-marine dolomite. In contrast, higher values (-0.7 to +0.1‰) were reported for recent sabkha dolomite in Abu Dhabi (Geske et al., 2015b). Li et al. (2015) suggested a temperature-dependence equation for $\Delta^{26}Mg_{dol\text{-}aq}$, based on experiments at high temperatures:

$$\Delta^{26}Mg_{dol\text{-}aq} = -0.1554(\pm 0.0096) \times 10^6/T^2, \quad (1)$$

where $\Delta^{26}Mg_{dol\text{-}aq}$ is the isotope difference between a dolomite and its forming solution and T is the temperature in Kelvin. Extrapolation of this equation to low-temperatures yields a $\Delta^{26}Mg_{dol\text{-}aq}$ in accordance with that suggested for deep-sea dolomite (Higgins and Schrag, 2010), but different from a previous sabkha study (Geske et al., 2015b). Theoretical calculations predict fractionation factors that are different from each other and from the experimental and natural data (Rustad et al., 2010; Schauble, 2011).

To evaluate factors determining the Mg isotope signature of dolomite, we studied pore-water and sediment from Dohat Faishakh Sabkha, Qatar. This coastal sabkha is among the very few environments in which dolomite is currently forming (e.g., Illing et al., 1965). This sabkha is an ideal 'natural laboratory' because: 1) sediment contamination from aeolian particles is minimal due to a location protected from the wind; 2) dolomite content in the sediment is high, up to 80-90% (e.g., Illing and Taylor, 1993) and 3) dolomite occurs in association with evaporitic minerals (aragonite, gypsum), which are often found in ancient sedimentary dolomite sequences (Wells, 1962).

GEOLOGICAL SETTING AND METHODS

Dohat Faishakh Sabkha is a marine evaporitic tidal-flat on the western coast of the Qatar peninsula, and includes a lagoon, an intertidal zone and a supratidal zone (Fig. 1; Illing et al., 1965; Illing and Taylor, 1993; Al-Disi et al., 2017). Most of the sediment in the lagoon and the intertidal zone is comprised of authigenic aragonite. The supratidal flats are the most saline zone, with authigenic dolomite and gypsum as the main sediments (e.g., Illing et al., 1965). The surface of the intertidal zone is fully colonized by microbial mats, which are also

present, gradually degraded toward the land, below the surface of the supratidal zone (Brauchli et al., 2016). These mats have been suggested to play an important role in the formation of dolomite (Bontognali et al., 2010; Brauchli et al., 2016). Lagoon water occasionally floods the supratidal zone, partly evaporates, and infiltrates the sediment. Lateral flow back to the lagoon is likely to take place (Illing and Taylor, 1993). Sediment temperature is 32±6°C (Müller et al., 2019).

Sediment cores of ~0.5m each were taken at three sites: DFn1, DF_{BM}, and DFn3 (Fig. 1C and Table SI1). Pore-water and lagoon water were extracted immediately after the collection of the cores in the field, using Rhizon devices. Cores and pore-water samples were then stored at ca. 4°C. Site DFn1 was sampled during three trips to identify seasonal variations. The sediment cores were sampled in the laboratory (Table SI3) and powdered. Then, ~20mg of each sample was used for XRD analysis. Selected samples, in which dolomite comprises ≥58% of the carbonates, were used for Mg isotope analysis. In such samples, the bulk δ^{26}Mg can be considered as the dolomite signature because the Mg contribution from other minerals is small. Solid samples were washed first with milli-Q water, to remove soluble salts, and then dissolved in HNO_3. The methods used for chemical and isotope analyses followed those described in Shalev et al. (2018a; 2019), and are summarized in the SI.

RESULTS

Major cations, mineralogy and Mg isotope results are presented in Tables SI3-4. The lagoon water is about twice concentrated relative to seawater and the pore-water is more concentrated than the lagoon (Figs. 2A-B). No significant seasonal change in concentration is observed at site DFn1. Lowest concentrations are observed at site DFn3, in the intertidal zone. Mg concentration, [Mg], is highest at site DF_{BM} (supratidal zone) and generally

decreases with depth, whereas Na concentration, [Na], is highest at site DFn1 (supratidal zone) and is generally constant with depth (Fig. 2A-B). Mg isotopes are not fractionated in the lagoon, whereas all pore-water samples are enriched in ^{26}Mg, and all sediment samples are depleted in ^{26}Mg relative to the seawater source (Fig. 2C). A similar pore-water trend toward higher $\delta^{26}Mg$ values with depth is observed at sites DF_{BM} and DFn3, but not at DFn1, where the $\delta^{26}Mg$ values are generally constant. These trends are not reflected in the dolomite samples. No dolomite $\delta^{26}Mg$ values from DFn3 are reported in Figures 2-4 because the sediment at this site is mostly comprised of aragonite and does not contain dolomite (Table SI4).

DISCUSSION

The ^{26}Mg-enriched pore-water (Fig. 2C) indicates that dolomite formation at the Dohat Faishakh Sabkha is ongoing over the residence time of the pore-water. The contribution of isotopically heavy magnesium from silicate minerals (e.g., Teng, 2017) is expected to be negligible due to their low abundance in the sediment (Table SI4). Mg-evaporites, which may form a ^{26}Mg-depleted sink (e.g., kainite; Shalev et al., in rev.), are not expected to precipitate at such relatively low degrees of evaporation, within the gypsum facies (e.g., Shalev et al., 2018b). Indeed, they were not observed in XRD analyses. Aragonite and calcite may also form a ^{26}Mg-depleted sink (e.g., Wombacher et al., 2011; Mavromatis et al., 2013) but, due to their low Mg content, this Mg sink is relatively small. Furthermore, despite significant seasonality in rainfall, expected to dilute the pore-water during the rainy season, no seasonal change in concentration has been observed in the pore-water (Fig. 2A-B). This observation excludes potential contribution of Mg from runoff or shallow groundwater. The generally constant [Na] with depth (Fig. 2B) is also inconsistent

with a groundwater contribution. Therefore, it is concluded that seawater is the major source of Mg to the pore-water, and that sedimentary dolomite is the major sink.

The isotopic difference between sediment and pore-water samples at the same depth, $\Delta^{26}Mg_{sed\text{-}PW}$, is between -1.97‰ and -1.57‰ (Fig. 3A, except for one sample: -0.86‰). For most samples, this isotopic difference is in accordance with -1.84‰ $<\Delta^{26}Mg_{dol\text{-}aq}<$ -1.51‰ (Equation 1; Li et al., 2015), as expected for dolomite precipitating in the temperature range for these sites, 32±6°C (Müller et al., 2019). It should be noted, though, that the pore-water is not necessarily the precipitating solution of the dolomite present at the same depth. Indeed, the formation of dolomite likely required hundreds of years, while the pore-water values represent a snapshot. Therefore, $\Delta^{26}Mg_{sed\text{-}PW}$ is not necessarily expected to be equal to $\Delta^{26}Mg_{dol\text{-}aq}$. Despite this caveat, the good agreement between the measured and the expected fractionations suggests that temperature is the major factor determining the Mg isotope fractionation in this sabkha system, and that any vital, rate, or other effects play a minor role. The microbial mediation process proposed for explaining sabkha-type dolomite formation is not expected to cause a metabolism-related Mg isotope fractionation (Brauchli et al., 2016). Magnesium is not assimilated by microbes, which catalyze the incorporation of Mg into the carbonate mineral by producing EPS that promote dehydration of aqueous Mg^{2+} (Bontognali et al., 2014). It is, however, possible that the interactions between Mg^{2+} and the EPS cause an isotope fractionation that is in turn recorded in the dolomite. Our data suggest that such hypothetical EPS-related fractionation is limited or even absent.

The $\delta^{26}Mg$ values of pore-water from each site are linearly correlated with both ln[Mg], where the slope gives $\Delta^{26}Mg_{dol\text{-}aq}$ for a Rayleigh model, and 1/[Mg], which simulates binary mixing (Figs. 3B-C). Thus, we suggest that the $\delta^{26}Mg$ of pore-water evolved by Rayleigh distillation due to dolomite formation, and/or by mixing of such dolomite-forming solutions, from seawater that is evaporated to a different degree at each site. Since Mg is

conservative during seawater evaporation (as long as there is no dolomite or Mg-evaporite formation), [Mg] rises as evaporation progresses, while δ^{26}Mg does not change (blue arrow in Figs. 3B-C). Thus, for each site, the Mg concentration before the onset of dolomite formation can be calculated from the intersection between the correlation line and the marine δ^{26}Mg value (Figs. 3B-C). Then, a degree of evaporation of seawater (DE) can be calculated by:

$$DE = [Mg]_i/[Mg]_{SW}, \quad (2)$$

where i and SW are intersection and seawater, respectively. The results suggest that the DE is 6.6–6.7 at DFn3, 8.3–8.5 at DFn1, and 10.5–10.9 at DF_{BM}. This further suggests that the pore-water is evaporated to the gypsum – or beginning of halite – facies, supporting the lack of any Mg-evaporites.

At the DF_{BM} and DFn3 sites, the uppermost pore-water sample is the least evolved relative to the intersection and [Mg] decreases with depth, while the δ^{26}Mg value increases (Figs. 3B-C). Furthermore, the slope on the ln[Mg] diagram (-1.69±0.35‰ for DFn3 and -1.35±0.32‰ for DF_{BM}; Fig. 3B) is within the range expected from Rayleigh distillation, with an isotope fractionation as derived from equation 1 (Li et al., 2015), -1.84‰ to -1.51‰. This suggests progressive Mg loss to dolomite with downward percolation of evaporated seawater. However, it is also possible that the deep dolomite-forming pore-water mixes back with the pore-water from the upper parts of the sediment at each site. Unlike sites DF_{BM} and DFn3, [Mg] and δ^{26}Mg values at DFn1 show no specific trend with depth and the slope in Figure 3B is much less negative (-0.85±0.22‰). This might suggest that the uppermost pore-water at this site mixes with dolomite-forming pore-water from a different place in the sabkha, such as the DFn3 site (Fig. 3C). This further implies that there is no ongoing dolomite formation at

DFn1 and, consistently with its landward location in the regressive sedimentary system, that the dolomite at this site is older.

It can be concluded, then, that the $\delta^{26}Mg$ values of dolomites in the Dohat Faishakh Sabkha are determined by three factors: 1) the formation temperature of the dolomite, which determines the isotope fractionation factor (though minor vital, rate, or other effects cannot be ruled out); 2) the extent of prior Mg removal into dolomite from pore-water, which enriches the pore-water in ^{26}Mg via a 'Rayleigh effect'; and 3) the extent of mixing with less-evolved evaporated seawater, which lowers the $\delta^{26}Mg$ values of the pore-water back towards the seawater value. Thus, the dolomite with the lowest $\delta^{26}Mg$, which was precipitated from pore-water with the least Rayleigh-evolved $\delta^{26}Mg$, can be used for seawater reconstructions (though, it will always be a maximum limit for seawater $\delta^{26}Mg$). Indeed, applying this approach to the Dohat Faishakh Sabkha dolomite results in retrieval of the modern seawater value (Fig. SI2).

CONCLUSIONS

The dolomite in the Dohat Faishakh Sabkha, Qatar, derived its Mg from evaporated modern seawater. An isotope fractionation, $\Delta^{26}Mg_{dol\text{-}aq}$, of -1.84‰ to -1.51‰, as calculated by Equation 1 (Li et al., 2015) for the local temperature, is in accordance with the pore-water and sediment data. Mg loss into dolomite is shown to alter the [Mg] and $\delta^{26}Mg$ values of the pore-water, enriching it with ^{26}Mg by a 'Rayleigh effect'. Mixing of such altered pore-water with unaltered evaporated seawater may reduce this ^{26}Mg-enrichment, but $\delta^{26}Mg$ values never go below the value of the original seawater (-0.83‰). Thus, it is concluded that, provided the lowest $\delta^{26}Mg$ value among several dolomite samples from the same system is used and the formation temperature is known, dolomite can be utilized as an archive for $\delta^{26}Mg$ values of ancient seawater. Also, tools such as Ca isotopes (e.g., Higgins et al., 2018),

can be used to trace the extent of Rayleigh distillation. Lastly, to use this approach, some preliminary conditions, which are met in the Dohat Faishakh Sabkha, should apply: 1) seawater is the major source of Mg to the system; 2) no Mg-evaporites present; and 3) dolomite is the major carbonate phase in the samples used.

ACKNOWLEDGMENTS

This study was funded by an SNSF Ambizione Grant PZ00P2_185988 to N.S. and SNSF grant 200021_184873/1 to D.V.

REFERENCES CITED

Azmy, K., Lavoie, D., Wang, Z., Brand, U., Al-Aasm, I., Jackson, S., and Girard, I., 2013, Magnesium-isotope and REE compositions of Lower Ordovician carbonates from eastern Laurentia: Implications for the origin of dolomites and limestones: Chemical Geology, v. 356, p. 64–75, doi: 10.1016/j.chemgeo.2013.07.015.

Blättler, C.L., Miller, N.R., and Higgins, J.A., 2015, Mg and Ca isotope signatures of authigenic dolomite in siliceous deep-sea sediments: Earth and Planetary Science Letters, v. 419, p. 32–42, doi: 10.1016/j.epsl.2015.03.006.

Bontognali, T.R.R., Mckenzie, J.A., Warthmann, R.J., and Vasconcelos, C., 2014, Microbially influenced formation of Mg-calcite and Ca-dolomite in the presence of exopolymeric substances produced by sulphate-reducing bacteria: Terra Nova, v. 26, p. 72–77, doi: 10.1111/ter.12072.

Bontognali, T.R.R., Vasconcelos, C., Warthmann, R.J., Bernasconi, S.M., Dupraz, C., Strohmenger, C.J., and Mckenzie, J.A., 2010, Dolomite formation within microbial mats in the coastal sabkha of Abu Dhabi (United Arab Emirates): Sedimentology, v. 57, p. 824–844, doi: 10.1111/j.1365-3091.2009.01121.x.

234 Brauchli, M., McKenzie, J.A., Strohmenger, C.J., Sadooni, F., Vasconcelos, C., and
235 Bontognali, T.R.R., 2016, The importance of microbial mats for dolomite formation
236 in the Dohat Faishakh sabkha, Qatar: Carbonates and Evaporites, v. 31, p. 339–345,
237 doi: 10.1007/s13146-015-0275-0.
238 Al Disi, Z.A., Jaoua, S., Bontognali, T.R.R., Attia, E.S.M., Al-Kuwari, H.A.A.S., and Zouari,
239 N., 2017, Evidence of a Role for Aerobic Bacteria in High Magnesium Carbonate
240 Formation in the Evaporitic Environment of Dohat Faishakh Sabkha in Qatar:
241 Frontiers in Environmental Science, v. 5, doi: 10.3389/fenvs.2017.00001.
242 Elderfield, H., 2010, Seawater chemistry and climate: Science, v. 327, p. 1092–1093, doi:
243 10.1126/science.1186769.
244 Geske, A., Goldstein, R.H., Mavromatis, V., Richter, D.K., Buhl, D., Kluge, T., John, C.M.,
245 and Immenhauser, A., 2015, The magnesium isotope (δ^{26}Mg) signature of dolomites:
246 Geochimica et Cosmochimica Acta, v. 149, p. 131–151, doi:
247 10.1016/j.gca.2014.11.003.
248 Geske, A., Lokier, S., Dietzel, M., Richter, D.K., Buhl, D., and Immenhauser, A., 2015,
249 Magnesium isotope composition of sabkha porewater and related (Sub-)Recent
250 stoichiometric dolomites, Abu Dhabi (UAE): Chemical Geology, v. 393–394, p. 112–
251 124, doi: 10.1016/j.chemgeo.2014.11.020.
252 Geske, A., Zorlu, J., Richter, D.K., Buhl, D., Niedermayr, A., and Immenhauser, A., 2012,
253 Impact of diagenesis and low grade metamorphosis on isotope (δ^{26}Mg, δ^{13}C, δ^{18}O and
254 ^{87}Sr/^{86}Sr) and elemental (Ca, Mg, Mn, Fe and Sr) signatures of Triassic sabkha
255 dolomites: Chemical Geology, v. 332–333, p. 45–64, doi:
256 10.1016/j.chemgeo.2012.09.014.

Gothmann, A.M., Stolarski, J., Adkins, J.F., and Higgins, J.A., 2017, A Cenozoic record of seawater Mg isotopes in well-preserved fossil corals: Geology, v. 45, p. 1039–1042, doi: 10.1130/G39418.1.

Higgins, J.A., Blättler, C.L., Lundstrom, E.A., Santiago-Ramos, D.P., Akhtar, A.A., Crüger Ahm, A.S., Bialik, O., Holmden, C., Bradbury, H., Murray, S.T., and Swart, P.K., 2018, Mineralogy, early marine diagenesis, and the chemistry of shallow-water carbonate sediments: Geochimica et Cosmochimica Acta, v. 220, p. 512–534, doi: 10.1016/j.gca.2017.09.046.

Higgins, J.A., and Schrag, D.P., 2010, Constraining magnesium cycling in marine sediments using magnesium isotopes: Geochimica et Cosmochimica Acta, v. 74, p. 5039–5053, doi: 10.1016/j.gca.2010.05.019.

Higgins, J.A., and Schrag, D.P., 2015, The Mg isotopic composition of Cenozoic seawater - evidence for a link between Mg-clays, seawater Mg/Ca, and climate: Earth and Planetary Science Letters, v. 416, p. 73–81, doi: 10.1016/j.epsl.2015.01.003.

Hu, Z., Hu, W., Wang, X., Lu, Y., Wang, L., Liao, Z., and Li, W., 2017, Resetting of Mg isotopes between calcite and dolomite during burial metamorphism : Outlook of Mg isotopes as geothermometer and seawater proxy: v. 208, p. 24–40, doi: 10.1016/j.gca.2017.03.026.

Illing, L.V., and Taylor, J.C.M., 1993, Penecontemporaneous dolomitization in Sabkha Faishakh, Qatar: evidence from changes in the chemistry of the interstitial brines: Journal of Sedimentary Petrology, v. 63, p. 1042–1048, doi: 10.1306/D4267C8F-2B26-11D7-8648000102C1865D.

Illing, L.V., Wells, A.J., and Taylor, J.C.M., 1965, Penecontemporary Dolomite in the Persian Gulf, in Dolomitization and Limestone Diagenesis, p. 89–111, doi: 10.2110/pec.65.07.0089.

Li, W., Beard, B.L., and Johnson, C.M., 2011, Exchange and fractionation of Mg isotopes between epsomite and saturated $MgSO_4$ solution: Geochimica et Cosmochimica Acta, v. 75, p. 1814–1828, doi: 10.1016/j.gca.2011.01.023.

Li, W., Beard, B.L., Li, C., Xu, H., and Johnson, C.M., 2015, Experimental calibration of Mg isotope fractionation between dolomite and aqueous solution and its geological implications: Geochimica et Cosmochimica Acta, v. 157, p. 164–181, doi: 10.1016/j.gca.2015.02.024.

Mavromatis, V., Gautier, Q., Bosc, O., and Schott, J., 2013, Kinetics of Mg partition and Mg stable isotope fractionation during its incorporation in calcite: Geochimica et Cosmochimica Acta, v. 114, p. 188–203, doi: 10.1016/j.gca.2013.03.024.

Müller, I.A., Rodriguez-Blanco, J.D., Storck, J.C., do Nascimento, G.S., Bontognali, T.R.R., Vasconcelos, C., Benning, L.G., and Bernasconi, S.M., 2019, Calibration of the oxygen and clumped isotope thermometers for (proto-)dolomite based on synthetic and natural carbonates: Chemical Geology, v. 525, p. 1–17, doi: 10.1016/j.chemgeo.2019.07.014.

Petrash, D.A., Bialik, O.M., Bontognali, T.R.R., Vasconcelos, C., Roberts, J.A., McKenzie, J.A., and Konhauser, K.O., 2017, Microbially catalyzed dolomite formation: From near-surface to burial: Earth-Science Reviews, v. 171, p. 558–582, doi: 10.1016/j.earscirev.2017.06.015.

Pogge Von Strandmann, P.A.E., Forshaw, J., and Schmidt, D.N., 2014, Modern and Cenozoic records of seawater magnesium from foraminiferal Mg isotopes: Biogeosciences, v. 11, p. 5155–5168, doi: 10.5194/bg-11-5155-2014.

Rustad, J.R., Casey, W.H., Yin, Q.-Z., Bylaska, E.J., Felmy, A.R., Bogatko, S. a., Jackson, V.E., and Dixon, D. a., 2010, Isotopic fractionation of Mg2+(aq), Ca2+(aq), and

306 Fe2+(aq) with carbonate minerals: Geochimica et Cosmochimica Acta, v. 74, p.
307 6301–6323, doi: 10.1016/j.gca.2010.08.018.
308 Schauble, E.A., 2011, First-principles estimates of equilibrium magnesium isotope
309 fractionation in silicate, oxide, carbonate and hexaaquamagnesium(2+) crystals:
310 Geochimica et Cosmochimica Acta, v. 75, p. 844–869, doi:
311 10.1016/j.gca.2010.09.044.
312 Schott, J., Mavromatis, V., Fujii, T., Pearce, C.R., and Oelkers, E.H., 2016, The control of
313 carbonate mineral Mg isotope composition by aqueous speciation: Theoretical and
314 experimental modeling: Chemical Geology, v. 445, p. 120–134, doi:
315 10.1016/j.chemgeo.2016.03.011.
316 Shalev, N., Bontognali, T.R.R., Wheat, C.G., and Vance, D., 2019, New isotope constraints
317 on the Mg oceanic budget point to cryptic modern dolomite formation: Nature
318 Communications, v. 10, p. 5646, doi: https://doi.org/10.1038/s41467-019-13514-6.
319 Shalev, N., Farkaš, J., Fietzke, J., Novák, M., Schuessler, J.A., Pogge von Strandmann,
320 P.A.E., and Törber, P.B., 2018, Mg Isotope Interlaboratory Comparison of Reference
321 Materials from Earth-Surface Low-Temperature Environments: Geostandards and
322 Geoanalytical Research, v. 42, p. 205–221, doi: 10.1111/ggr.12208.
323 Shalev, N., Lazar, B., Halicz, L., and Gavrieli, I. The Mg isotope signature of marine Mg-K-
324 evaporites: Geochimica et Cosmochimica Acta, v. In Review.
325 Shalev, N., Lazar, B., Köbberich, M., Halicz, L., and Gavrieli, I., 2018, The chemical
326 evolution of brine and Mg-K-salts along the course of extreme evaporation of
327 seawater – An experimental study: Geochimica et Cosmochimica Acta, v. 241, p.
328 164–179, doi: 10.1016/J.GCA.2018.09.003.
329 Teng, F.-Z., 2017, Magnesium Isotope Geochemistry: Reviews in Mineralogy and
330 Geochemistry, v. 82, p. 219–287, doi: 10.2138/rmg.2017.82.7.

Tipper, E.T., Galy, A., Gaillardet, J., Bickle, M.J., Elderfield, H., and Carder, E.A., 2006, The magnesium isotope budget of the modern ocean: Constraints from riverine magnesium isotope ratios: Earth and Planetary Science Letters, v. 250, p. 241–253, doi: 10.1016/j.epsl.2006.07.037.

Wells, A.J., 1962, Recent dolomite in the Persian Gulf: Nature, v. 194, p. 274–275, doi: 10.1038/194274a0.

Wombacher, F., Eisenhauer, A., Böhm, F., Gussone, N., Regenberg, M., Dullo, W.C., and Rüggeberg, A., 2011, Magnesium stable isotope fractionation in marine biogenic calcite and aragonite: Geochimica et Cosmochimica Acta, v. 75, p. 5797–5818, doi: 10.1016/j.gca.2011.07.017.

FIGURE CAPTIONS

Figure 1. Geological setting of Dohat Faishakh Sabkha. (A) Location map. (B) Schematic illustration of the geological setting (after: Illing and Taylor, 1993). (C) Sampling sites (red points) are distributed along the transect originally studied by Illing et al. (1965). The sites studied by Brauchli et al. (2016) are also shown (white arrow). Satellite images from ©2019 Google (Imagery ©2019 CNES/ Airbus, Maxar Tech., Map data ©2019).

Figure 2. Depth profiles of pore water (PW) and sediment (SED). Colors: DFn1 – green, DF_{BM} – orange, DFn3 – grey, Lagoon – cyan square, Seawater – vertical blue line. A) and B) [Mg] and [Na] in water samples. DFn1 sampling trips: green (3/2016), yellow (11/2016), and blue (2/2017). Error bars are 5% analytical error. C) $\delta^{26}Mg$ values of pore-water (solid circles) and sediment (empty diamonds). Error bars are 2SD.

355 Figure 3. $\delta^{26}Mg$ values in the Dohat Faishakh Sabkha. A) Isotopic difference between
356 dolomite and pore-water samples at the same depth, $\Delta^{26}Mg_{sed\text{-}PW}$. Error bars are propagated
357 2SD. Black lines show the expected fractionation for 32±6°C (equation 1; Li et al., 2015),
358 with its uncertainty (dotted lines). B) and C) Pore-water $\delta^{26}Mg$ values vs. ln[Mg] and 1/[Mg],
359 respectively. DFn1 – green, DF_{BM} – orange, DFn3 – grey. Error bars are 2SD. A linear
360 correlation (colored solid line; ±SE shown as dashed lines), Y=aX+b, is shown for each site
361 (a and b are indicated with 95% confidence limits in parenthesis). One outlier, with the
362 largest error, is not considered in the correlation for site DFn1. Seawater (SW) and the lagoon
363 water results are shown by the black arrow. The seawater evaporation trend, without any
364 dolomite formation, is shown by a blue arrow. $[Mg]_i$ is the Mg concentration (in mM) at the
365 intersection of the correlation and the evaporation lines.
366
367
368 [1]GSA Data Repository item 201Xxxx, Mg isotope measurements details, Supplementary
369 Figures SI1-2, and Supplementary Tables SI1-4, is available online at
370 www.geosociety.org/pubs/ft20XX.htm, or on request from editing@geosociety.org.
371

Fig. 1:

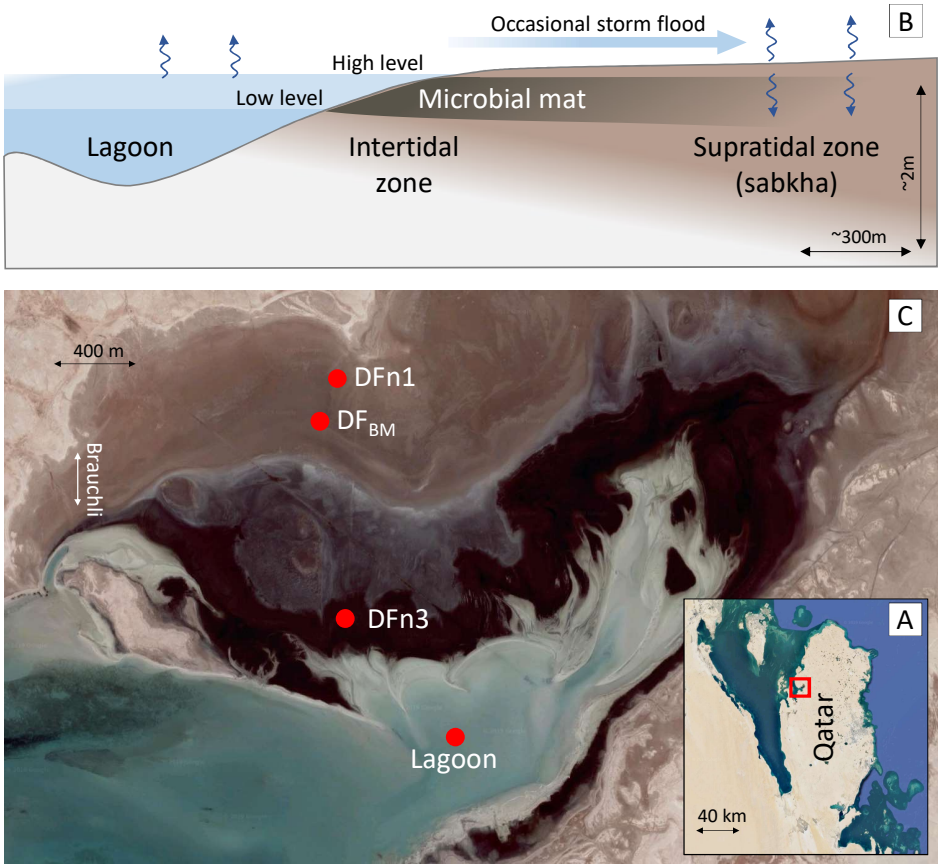
B
Occasional storm flood
High level
Low level
Microbial mat
Lagoon
Intertidal zone
Supratidal zone (sabkha)
~2m
~300m
C
400 m
DFn1
DF$_{BM}$
Brauchli
DFn3
Lagoon
A
Qatar
40 km

Fig. 2

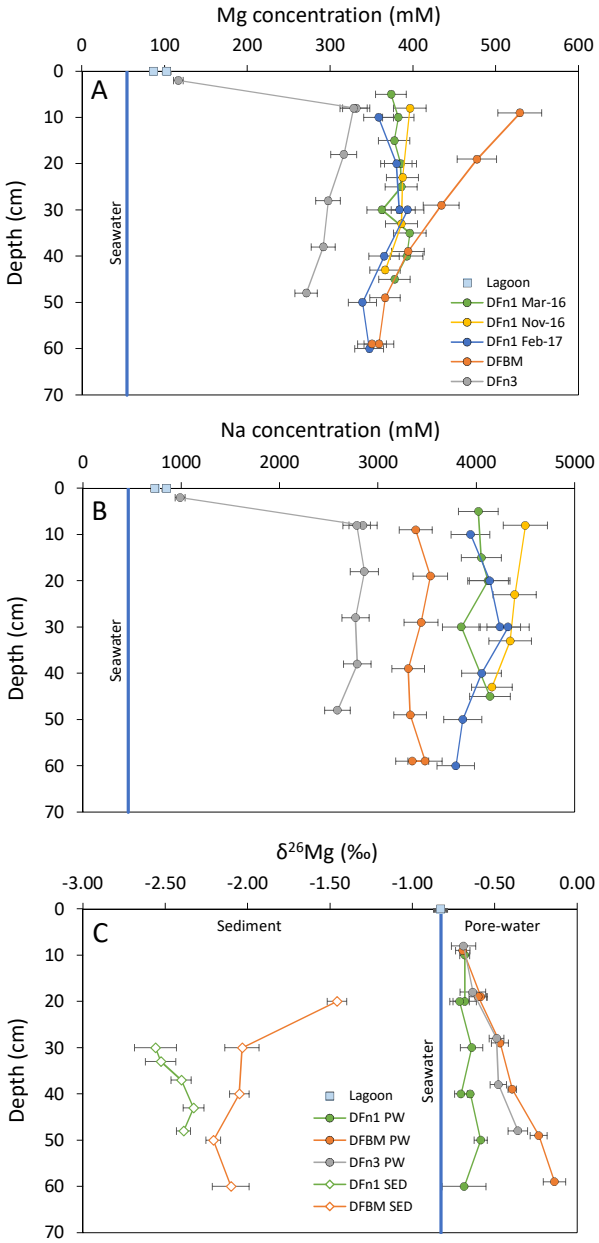
Mg concentration (mM)
0
100
200
300
400
500
600
A
Depth (cm)
Seawater
Lagoon
DFn1 Mar-16
DFn1 Nov-16
DFn1 Feb-17
DFBM
DFn3
Na concentration (mM)
0
1000
2000
3000
4000
5000
B
δ26Mg (‰)
-3.00
-2.50
-2.00
-1.50
-1.00
-0.50
0.00
C
Sediment
Pore-water
Lagoon
DFn1 PW
DFBM PW
DFn3 PW
DFn1 SED
DFBM SED

Fig. 3

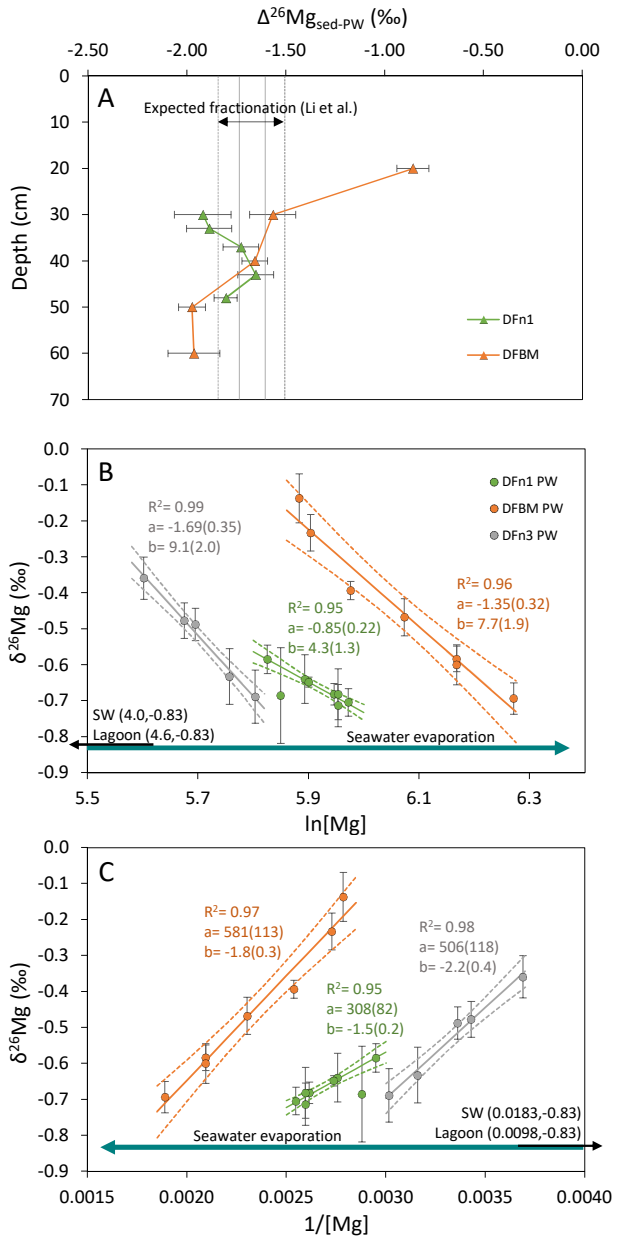
Δ26Mgsed-PW (‰)
-2.50
-2.00
-1.50
-1.00
-0.50
0.00
A
Expected fractionation (Li et al.)
Depth (cm)
DFn1
DFBM
B
DFn1 PW
DFBM PW
DFn3 PW
R²= 0.99
a= -1.69(0.35)
b= 9.1(2.0)
R²= 0.95
a= -0.85(0.22)
b= 4.3(1.3)
R²= 0.96
a= -1.35(0.32)
b= 7.7(1.9)
SW (4.0,-0.83)
Lagoon (4.6,-0.83)
Seawater evaporation
δ26Mg (‰)
ln[Mg]
C
R²= 0.97
a= 581(113)
b= -1.8(0.3)
R²= 0.98
a= 506(118)
b= -2.2(0.4)
R²= 0.95
a= 308(82)
b= -1.5(0.2)
Seawater evaporation
SW (0.0183,-0.83)
Lagoon (0.0098,-0.83)
δ26Mg (‰)
1/[Mg]

Sabkha Dolomite as an Archive for the Magnesium Isotope Composition of Seawater

Supplementary Information

Netta Shalev[1], Tomaso R.R. Bontognali[123], and Derek Vance[1]

[1]Institute of Geochemistry and Petrology, Department of Earth Sciences, ETH Zürich, Clausiusstrasse 25, 8092 Zürich, Switzerland; netta.shalev@erdw.ethz.ch

[2] Space Exploration Institute, Fbg de l'Hopital 68, 2002 Neuchâtel, Switzerland

[3]Department of Environmental Sciences, University of Basel, Klingelbergstrasse 27, Basel, Switzerland

SUPPLEMENTARY INFORMATION

Mg Isotope Measurements

XRD analyses were done using a Bruker AXS D8 Advance Diffractometer. There was no further preparation of the pore-water samples, except for the Mg column chemistry described below. Concentrations were measured on a Thermo Scientific Element XR ICP-MS. Mg was purified using 0.5M and 2.0M HCl on Bio-Rad AG® 50W-X12 (200–400 mesh) resin in 30 ml Savillex Microcolumns. A yield of close to 100% and a total matrix element/Mg ratio of <0.05 were measured for each sample. Magnesium isotope ratios were measured on a Thermo Scientific Neptune MC-ICP-MS using a standard-sample bracketing method. The δ^{26}Mg values are reported relative to DSM3. Results of pure Mg solutions and natural reference materials are identical within error to the values reported in the literature (Suppl. Table 2; e.g., Foster et al., 2010; Ling et al., 2011; An and Huang, 2014, Shalev et al., 2018a). The δ^{25}Mg versus δ^{26}Mg results determined in this study plot on a single line with a slope of 0.512 (Suppl. Figure 1), suggesting no major influence of isobaric interferences on the measured Mg isotope ratios.

Supplementary Figures

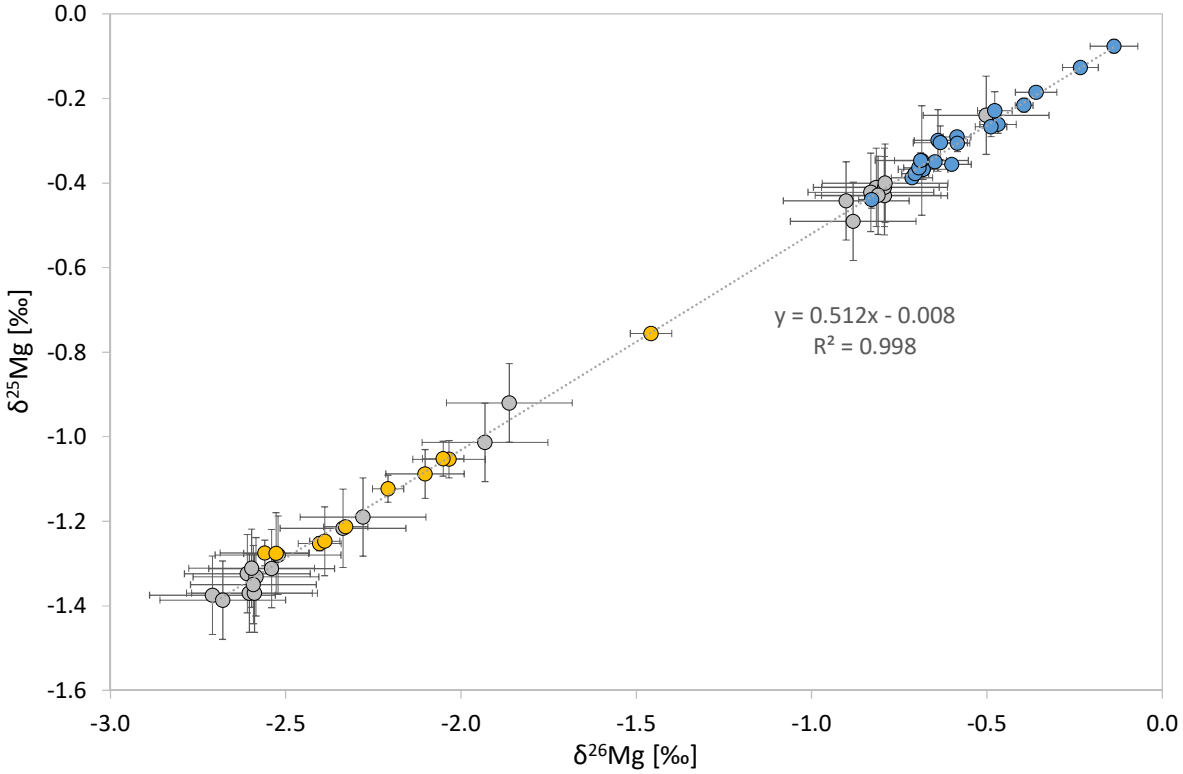

Supplementary Figure 1. $\delta^{25}Mg$ versus $\delta^{26}Mg$ values of samples and reference materials measured in this study. Data from Supplementary Tables 2-4. Grey – reference materials; Blue – pore water samples from DFS; Yellow – sediment samples from DFS. Error bars are 2SD of each result. The data are in accordance with a regression line (dotted) that crosses close to the origin and has a slope of 0.512, typical of mass dependent fractionation of terrestrial material.

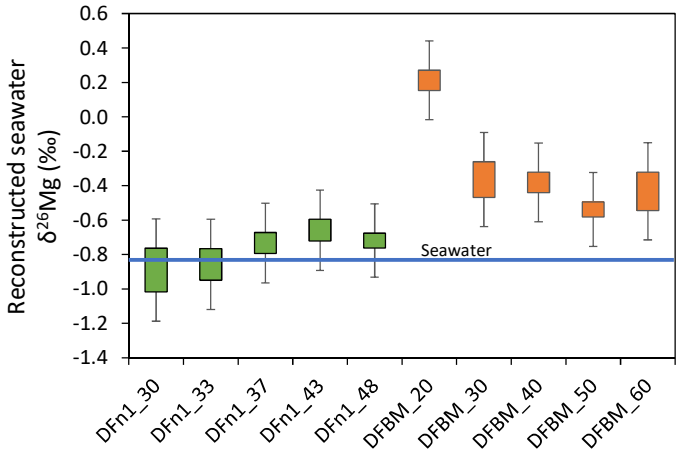

Supplementary Figure 2. Reconstructed $\delta^{26}Mg$ values of seawater as calculated from DFS dolomites. Colors: DFn1 – green; DF_{BM} – orange; True seawater – blue line. An isotope fractionation of -1.67‰ (for 32°C, in equation 1; Li et al., 2015) was used. Boxes indicate the results within the 2SD on the $\delta^{26}Mg$ of the dolomite. Error bars show the further uncertainty results from the uncertainty on the temperature (±6°C).

Supplementary Tables

Supplementary Table 1: Core sampling sites location

Core	Latitude	Longitude
DFn1	25°38'13.4"N	50°57'31.9"E
DFn3	25°37'31.5"N	50°57'39.2"E
DF_{BM}	25°38'05.4"N	50°57'35.3"E

Supplementary Table 2: Mg isotope results of reference materials processed through the same Mg separation and instrumental procedures as the samples.

Material and replicate [a]	δ^{26}Mg (‰)	2SD (‰)	δ^{25}Mg (‰)	2SD (‰)	n
DSM3					
Pure Mg passed through column	0.00	0.06	0.01	0.04	4
Cambridge-1					
A	-2.60	0.21	-1.37	0.20	3
B	-2.59	0.08	-1.37	0.13	4
C	-2.52	0.08	-1.28	0.08	3
D	-2.54	0.05	-1.31	0.02	4
E	-2.61	0.18	-1.32	0.22	4
F	-2.58	0.09	-1.33	0.11	4
G	-2.60	0.21	-1.31	0.22	4
H	-2.71	0.11	-1.37	0.02	4
I	-2.68	0.07	-1.39	0.02	3
Pure Mg passed through column	-2.59	0.10	-1.35	0.12	4
Average	**-2.60**	**0.11**	**-1.34**	**0.07**	**10**
Literature [b]	**-2.61**	**0.05**	**-1.34**	**0.04**	
Seawater					
A	-0.82	0.06	-0.41	0.03	4
B	-0.79	0.13	-0.43	0.13	4
C	-0.79	0.06	-0.41	0.09	4
D	-0.79	0.05	-0.40	0.05	4
E	-0.83	0.14	-0.42	0.18	4
F	-0.81	0.08	-0.43	0.14	8
G	-0.90	0.08	-0.44	0.02	4
H	-0.88	0.11	-0.49	0.03	4
Average	**-0.83**	**0.09**	**-0.43**	**0.06**	**8**
Literature [c]	**-0.83**	**0.09**	**-0.43**	**0.06**	**90**
Jdo-1 Dolomite					
A	-2.28	0.06	-1.19	0.05	4
B	-2.34	0.09	-1.22	0.09	4
Literature [d]	**-2.35**	**0.15**	**-1.23**	**0.09**	**11**
CRM-512 dolomite					
A	-1.86	0.09	-0.92	0.11	4
B	-1.93	0.02	-1.01	0.02	4
Literature [d]	**-2.03**	**0.17**	**-1.05**	**0.09**	**6**
DSW-1					
Dead Sea brine	-0.50	0.08	-0.24	0.10	4
Literature [d]	**-0.58**	**0.12**	**-0.30**	**0.07**	**8**

[a] Different column chemistry replicates are indicated by A-H, except for replicates A-I of the pure Mg Cambridge-1, which include the MC-ICP-MS measurements only; [b] An and Huang (2014), Shalev et al. (2018a); [c] Ling et al. (2011); [d] Shalev et al. (2018).

Supplementary Table 3: Major cations concentrations and Mg isotope results of pore water from DFS.

			Major cations				Mg isotopes				
Location	**Sampl. date**	**Depth**	**Na**	**Mg**	**K**	**Ca**	**δ^{26}Mg**	**2SD**	**δ^{25}Mg**	**2SD**	**n**
		cm	mM	mM	mM	mM	‰	‰	‰	‰	
Seawater[a]			460	55	11	11	-0.83	0.09	-0.43	0.06	8
Lagoon water	Mar-16	0	847	103	17	22	-0.83	0.04	-0.44	0.02	4
Lagoon water	Nov-17	0	731	86	15	18					
DFn1	Mar-16	5	4021	373	64	27					
DFn1	Mar-16	10	n.a.	382	67	25	-0.68	0.03	-0.37	0.01	4
DFn1	Mar-16	15	4051	377	64	28					
DFn1	Mar-16	20	4120	385	62	26	-0.68	0.07	-0.37	0.02	4
DFn1[b]							-0.71	0.06	-0.39	0.01	4
DFn1	Mar-16	25	n.a.	386	69	24					
DFn1	Mar-16	30	3847	363	63	26	-0.64	0.07	-0.30	0.07	2
DFn1	Mar-16	35	n.a.	396	71	23					
DFn1	Mar-16	40	n.a.	392	69	23	-0.70	0.04	-0.38	0.01	4
DFn1	Mar-16	45	4138	378	62	26					
DFn1	Nov-16	8	4498	396	70	29					
DFn1	Nov-16	23	4392	388	72	28					
DFn1	Nov-16	33	4345	386	71	28					
DFn1	Nov-16	43	4159	366	70	30					
DFn1	Feb-17	10	3942	359	65	24					
DFn1	Feb-17	20	4137	380	68	24					
DFn1	Feb-17	30	4239	384	66	24					
DFn1[b]	Feb-17	30	4323	394	68	24					
DFn1	Feb-17	40	4054	365	66	26	-0.65	0.01	-0.35	0.01	4
DFn1	Feb-17	50	3862	339	64	29	-0.59	0.04	-0.29	0.01	4
DFn1	Feb-17	60	3792	347	61	27	-0.69	0.13	-0.35	0.13	4
DF_{BM}	Nov-17	9	3384	529	79	15	-0.69	0.04	-0.36	0.02	4
DF_{BM}	Nov-17	19	3533	477	81	20	-0.58	0.04	-0.31	0.02	4
DF_{BM}[b]							-0.60	0.06	-0.36	0.01	3
DF_{BM}	Nov-17	29	3439	434	81	26	-0.47	0.05	-0.26	0.02	4
DF_{BM}	Nov-17	39	3308	394	73	31	-0.39	0.03	-0.22	0.02	4
DF_{BM}	Nov-17	49	3328	366	78	41	-0.23	0.05	-0.13	0.01	3
DF_{BM}	Nov-17	59	3479	359	80	50	-0.14	0.07	-0.08	0.02	3
DF_{BM}[b]	Nov-17	59	3348	351	74	52					
DFn3 (inside mat)	Nov-17	2	988	117	18	24					
DFn3	Nov-17	8	2849	332	53	25	-0.69	0.07	-0.35	0.02	4
DFn3[b]	Nov-17	8	2785	328	53	24					
DFn3	Nov-17	18	2862	316	56	27	-0.63	0.08	-0.30	0.04	4
DFn3	Nov-17	28	2772	298	53	30	-0.49	0.04	-0.27	0.02	4
DFn3	Nov-17	38	2790	292	51	33	-0.48	0.05	-0.23	0.05	4
DFn3	Nov-17	48	2588	271	52	34	-0.36	0.06	-0.19	0.01	4

n.a. not analyzed; [a] Seawater concentration data from Riley & Chester (1971); isotope data from current study; [b] Replicate.

Supplementary Table 4: Mineralogy and Mg isotope composition of sediments from DFS. Dol – dolomite, Ara – aragonite, Cal – calcite, Gyp – gypsum, Hal – halite, Q – quartz.

		Mineralogy						Mg isotopes				
Location	**Depth**	**Dol**	**Ara**	**Cal**	**Gyp**	**Hal** [a]	**Q**	**δ^{26}Mg**	**2SD**	**δ^{25}Mg**	**2SD**	**n**
	cm	wt%	wt%	wt%	wt%	wt%	wt%	‰	‰	‰	‰	
DFn1	17	0	0	0	93	7	0					
DFn1[b]	17	0	0	10	90	0	0					
DFn1	30	48	0	0	21	30	0	-2.56	0.13	-1.27	0.03	4
DFn1	33	78	0	0	9	12	0	-2.53	0.09	-1.28	0.10	4
DFn1	37	80	0	0	6	14	0	-2.40	0.06	-1.25	0.02	4
DFn1	43	68	0	0	8	18	6	-2.33	0.06	-1.21	0.01	4
DFn1	48	83	4	0	0	11	3	-2.39	0.04	-1.25	0.08	4
DFn1[b]	48	79	6	0	0	16	0					
DFn1[c]	48	80	0	0	0	20	0					
DF_{BM}	10	0	0	16	47	37	0					
DF_{BM}	20	22	0	8	36	33	0	-1.46	0.06	-0.76	0.01	4
DF_{BM}	30	37	0	4	0	53	6	-2.03	0.10	-1.05	0.04	4
DF_{BM}	40	21	3	5	0	67	4	-2.05	0.06	-1.05	0.04	4
DF_{BM}	50	34	10	6	0	45	5	-2.21	0.04	-1.12	0.03	4
DF_{BM}	60	33	17	7	0	42	0	-2.10	0.11	-1.09	0.06	4
DF_{BM}[b]	60	35	17	0	0	48	0					
DFn3	14	0	71	0	0	29	0					
DFn3	34	0	73	0	0	27	0					

[a] Halite might be an artifact of the pore water evaporation that occurs in the laboratory.
[b] Duplicate.
[c] Replicate.

Supplementary References

An, Y., and Huang, F., 2014, A review of Mg isotope analytical methods by MC-ICP-MS: Journal of Earth Science, v. 25, p. 822–840, doi: 10.1007/s12583-014-0477-8.

Foster, G.L., Pogge Von Strandmann, P.A.E., and Rae, J.W.B., 2010, Boron and magnesium isotopic composition of seawater: Geochemistry, Geophysics, Geosystems, v. 11, p. 1–10, doi: 10.1029/2010GC003201.

Li, W., Beard, B.L., Li, C., Xu, H., and Johnson, C.M., 2015, Experimental calibration of Mg isotope fractionation between dolomite and aqueous solution and its geological implications: Geochimica et Cosmochimica Acta, v. 157, p. 164–181, doi: 10.1016/j.gca.2015.02.024.

Ling, M.X., Sedaghatpour, F., Teng, F.Z., Hays, P.D., Strauss, J., and Sun, W., 2011, Homogeneous magnesium isotopic composition of seawater: An excellent geostandard for Mg isotope analysis: Rapid Communications in Mass Spectrometry, v. 25, p. 2828–2836, doi: 10.1002/rcm.5172.

Riley, J., and Chester, R., 1971, Introduction to marine chemistry: New York, Academic.

Shalev, N., Farkaš, J., Fietzke, J., Novák, M., Schuessler, J.A., Pogge von Strandmann, P.A.E., and Törber, P.B., 2018, Mg Isotope Interlaboratory Comparison of Reference Materials from Earth-Surface Low-Temperature Environments: Geostandards and Geoanalytical Research, v. 42, p. 205–221, doi: 10.1111/ggr.12208.